ELECTRICAL, OPTICAL AND STRUCTURAL INVESTIGATION OF LOW-TEMPERATURE PECV-DEPOSITED HYDROGENATED AMORPHOUS SILICON-OXYNITRIDE FILMS FOR SURFACE PASSIVATION OF CRYSTALLINE SILICON SOLAR CELLS

Daniel Sommer, Nils Brinkmann, Gabriel Micard, Giso Hahn, Barbara Terheiden
University of Konstanz, Department of Physics, 78457 Konstanz, Germany
Phone: +49 (0) 7531 88 2132, Fax: +49 (0) 7531 88 3895, Email: daniel.sommer@uni-konstanz.de

ABSTRACT: Amorphous silicon oxynitride (a-SiO_xN_y:H) films, which are deposited by plasma enhanced chemical vapor deposition (PECVD) at low temperatures (T_{dep} < 200°C), are investigated in terms of their electrical, optical, and structural properties. The purpose is to develop a passivation layer for crystalline silicon solar cells, which is comparable to amorphous silicon (a-Si:H) films in terms of manufacturing process and passivation quality, but superior to a-Si:H films in terms of parasitic absorption. In comparison to a-Si:H films, amorphous silicon oxynitride films suffer less from parasitic absorption over the whole wavelength range due to their higher optical band gap (E_g). The widening of the optical band gap is realized by the incorporation of oxygen and nitrogen atoms in the amorphous network. Ongoing with the incorporation of oxygen and nitrogen atoms is the possibility to tune the refractive index (n) in a certain range, which turns amorphous silicon oxynitride into a very interesting material for solar cell applications, in particular for heterojunction solar cells and multilayer anti reflection coatings.
Keywords: PECVD, Lifetime, Absorption

1 INTRODUCTION

In the ongoing improvement process of crystalline silicon (c-Si) solar cells, wafer surface passivation has proven to be a key issue [1]. A high surface recombination velocity directly lowers open circuit voltage and thus cell efficiency [1]. With the production cost driven trend to decrease wafer thickness, surface passivation becomes even more important as the surface to volume ratio increases.

Intrinsic amorphous silicon deposited at low temperatures by plasma enhanced chemical vapor deposition (PECVD) is reported to provide excellent surface passivation quality [2]. The major drawback of a-Si:H films employed as heteroemitters or passivation layers on the front side of a solar cell is the strong parasitic absorption of light which causes a loss in the short circuit current [3]. The absorption within the a-Si:H films can be minimized by widening the optical band gap. This can be realized by the incorporation of for example carbon, nitrogen or oxygen in the amorphous matrix [4]. Whereas a lot of groups studied Si-rich amorphous silicon carbide (a-SiC_x:H) [5] and oxide (a-SiO_x:H) films [6] which feature a very good passivation quality compared to amorphous silicon, only little work is done investigating amorphous silicon oxynitride (a-SiO_xN_y:H) films in the field of photovoltaics, focusing mainly upon the application of intrinsic a-SiO_xN_y:H films as firing stable passivation stacks [7,8].

This work fundamentally examines the structure of a-SiO_xN_y:H films in order to correlate passivation quality and optical parameters with the composition of the films.

2 EXPERIMENTAL

The a-SiO_xN_y:H samples are manufactured by using a commercial PECVD unit (PlasmaLab 100 from Oxford Instruments) in a direct plasma system operating at a radio frequency (RF) of 13.56 MHz. The a-SiO_xN_y:H films are grown from a plasma consisting of silane (SiH_4), hydrogen (H_2), and nitrous oxide (N_2O). All nitrous oxide gas flows quoted in this work refer to their dilution ratio in silane $R_{N2O} = [N_2O]/([N_2O]+[SiH_4])$. The 250 µm thick 2 Ωcm boron-doped high quality float-zone (FZ) silicon wafers (100)-oriented with an area of 5x5cm² are prepared with a standard chemical polishing [9] followed by a RCA cleaning [10]. Prior to the PECV-deposition a diluted hydrofluoric acid solution (HF, 2%) for removing the native oxide is performed. After the deposition an annealing step in ambient air is needed to activate the layers. The characterisation of this material is split in three different manners: the electrical, the optical part and structure analysis. The electrical part, which means passivation quality of the a-SiO_xN_y:H films, is evaluated in terms of the effective minority carrier lifetime τ_{eff} of surface passivated crystalline silicon wafers. τ_{eff} is determined as a function of the excess carrier density by means of photoconductance decay (PCD) measurement (WCT 120 from Sinton Consulting Inc.) [11]. Using τ_{eff} evaluated at an excess carrier density of $\Delta n = 1 \times 10^{15}$ cm^{-3} the surface recombination velocity (S_{eff}) is calculated according to (assuming identical S_{eff} on both sides of the wafer) [12]

$$S_{eff} = \frac{W}{2}\left(\frac{1}{\tau_{eff}} - \frac{1}{\tau_{bulk}}\right) \quad (1)$$

with τ_{bulk} being carrier lifetime in the silicon bulk, and W denoting wafer thickness. For degradation experiments (Staebler-Wronski-Effect [13]) the lifetime samples are exposed to light from an approximately one sun black body radiator for 13.5 h at 50°C.

The thickness of the deposited films d_{film} and their optical properties are deduced from spectral ellipsometry measurements between 250 and 1000 nm. For this purpose the (ψ, Δ) data are fitted by a Kramers-Kronig-consistent model [14]. The optical band gap E_g is calculated from the fitted data by using Tauc's formula [15]

$$\alpha(\hbar\omega) \sim \frac{(\hbar\omega - E_g)^2}{\hbar\omega} \quad (2)$$

A qualitative bonding analysis of the a-SiO_xN_y:H films is performed by means of Fourier-transform infra-red spectroscopy (FTIR). The thickness of the deposited layers is in contrast to the lifetime samples on one side

higher (d_{film} >150 nm) and the other side is mechanically polished.

3 RESULTS

3.1 Passivation quality

a) Effect of deposition temperature and post deposition annealing

Independent of the deposition parameters, all c-Si floatzone (FZ) wafers (2 Ωcm p-type, thickness 250 µm) passivated by a-SiO_xN_y:H films show effective lifetime values which are lower than τ_{eff} <100 µs in the as-deposited state. However, effective minority carrier lifetime can be increased by subsequent annealing of the samples. An annealing temperature of 300°C is the optimum. Therefore, in the following all reported lifetime values are determined in the annealed state (10 min at 300°C). Initially, the a-SiO_xN_y:H films are deposited at various substrate temperatures in the range of 125-325°C with a N_2O to SiH_4 gas flow ratio of R_{N2O} = 20%. The best passivation quality is achieved at a deposition temperature of 175°C yielding τ_{eff} = 2.25 ms, which corresponds to S_{eff} = 5.25 cm/s (Fig. 1).

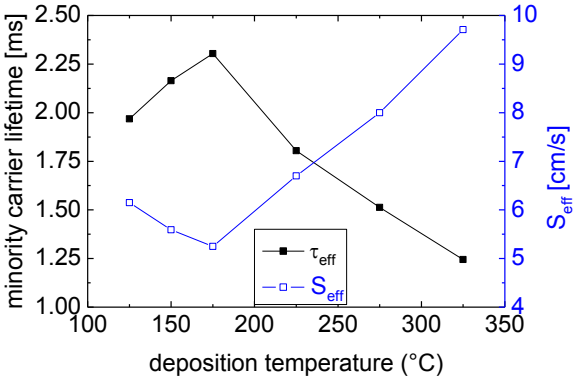

Figure 1: Effective minority carrier lifetime and surface recombination velocity of a-SiO_xN_y:H passivated c-Si FZ wafers as a function of deposition temperature at a N_2O gas flow ratio of 20%.

b) Effect of gas flow ratio R_{N2O}

It is observable that the effective minority carrier lifetime of a-SiO_xN_y:H passivated c-Si FZ wafers decreases linearly with increasing N_2O gas flow (Fig. 2). Without adding N_2O to the precursor gas, an effective lifetime value of 4.3 ms (S_{eff} = 2.9 cm/s) is achieved (see Fig. 2).

This very high effective lifetime is within the range of other values reported for c-Si FZ wafers which are passivated with amorphous silicon (a-Si:H) films [2]. When applying an a-SiO_xN_y:H film with an optical gap of 2.0 eV as passivation film, a still very high τ_{eff} of 2.5 ms (S_{eff} = 5 cm/s) is reached.

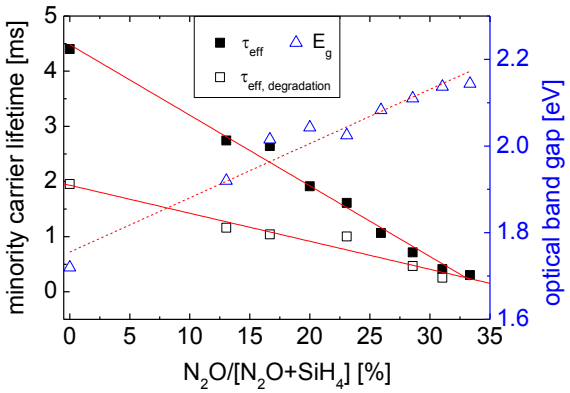

Figure 2: Effective minority carrier lifetime and optical band gap of a-SiO_xN_y:H films as a function of N_2O gas dilution ratio.

c) Effect of light induced degradation

Another issue, which is always connected to amorphous silicon, is its instability under illumination [13]. This light-induced degradation occurs in a-Si:H/c-Si structures by the creation of dangling-bonds [16]. To investigate the influence on the amorphous silicon oxynitrides, the lifetime samples are exposed to light from a black body radiator (1-Sun illumination for 13.5 h at 50°C). It is observed that the degradation reduces with increasing N_2O-dilution (Fig. 2). The degradation vanishes for a N_2O gas dilution ratio of about 30%.

3.2 Optical properties

a) Optical band gap

The optical band gap of amorphous silicon strongly depends on its atomic composition [4]. A widening can be achieved e.g. by adding carbon, nitrogen or oxygen into the amorphous matrix [5,6]. Therefore, the optical band gap of the deposited a-SiO_xN_y:H films widens with increasing N_2O gas dilution ratio (Fig. 2). It has to be noticed, that the optical band gap of the a-SiO_xN_y:H films depends linearly on the N_2O gas dilution ratio (R_{N2O} = 0-35%) as it is also the case for effective lifetime (see Fig. 2).

The optical band gap of films which are deposited without N_2O in the precursor gas mixture (R_{N2O} = 0%) is determined to be 1.72 eV, which is again in accordance with the values reported in literature for a-Si:H films [4]. The optical band gap widens to 2.15 eV for films deposited at R_{N2O} = 35%.

The widening of the optical band gap is accompanied by a decrease of the absorption coefficient resulting in a lower absorption within the a-SiO_xN_y:H films over the whole wavelength range compared to amorphous silicon (Fig. 3).

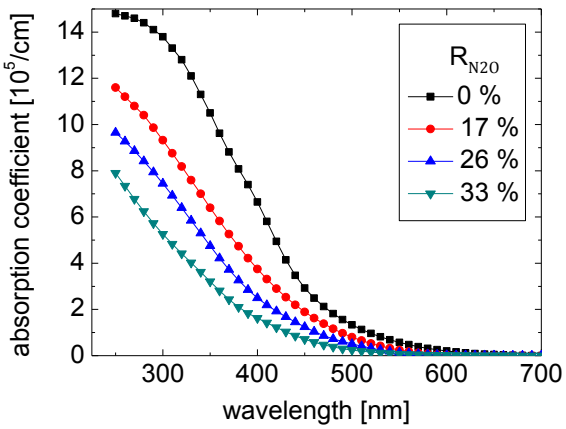

Figure 3: Spectral absorption coefficient α of a-SiO_xN_y:H films deposited at various N_2O gas dilution ratios.

b) Refractive index n

The refractive index n, evaluated at a wavelength of 600 nm, depends on the N_2O gas dilution ratio in a similar way as the optical band gap. Thus the refractive index decreases linearly with increasing N_2O dilution flow (Fig. 4), starting at n = 4.08 for the a-Si:H film (R_{N2O} = 0%). Note, that the refractive index of stoichiometric SiO_2 has been determined to 1.48 [17].

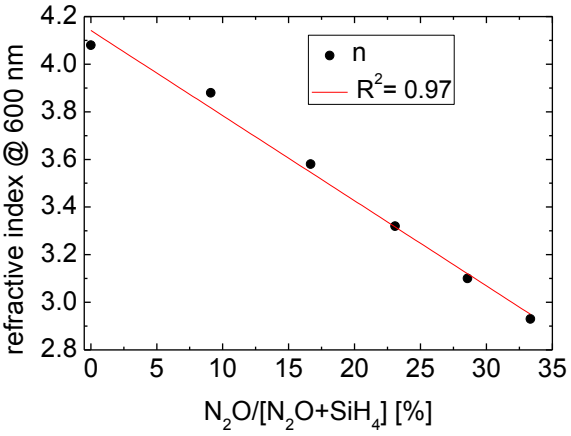

Figure 4: Refractive index (real part) n of a-SiO_xN_y:H films as a function of N_2O gas dilution ratio.

3.3 Compositional analysis

a) SIMS analysis

The concentrations of nitrogen and oxygen in some selected a-SiO_xN_y:H films are determined by means of Secondary-Ion Mass Spectroscopy measurements (SIMS) (Fig. 5).

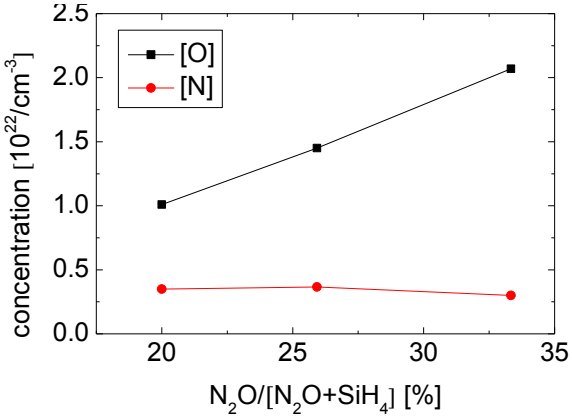

Figure 5: Oxygen and nitrogen concentration of a-SiO_xN_y:H films as a function of N_2O gas dilution ratio.

The concentration of nitrogen remains almost constant while increasing the N_2O gas dilution ratio (at least between R_{N2O} = 20 - 30%), whereas the oxygen concentration increases linearly. This dependence correlates with the linear increase of the optical band gap and the linear decrease of the effective lifetime τ_{eff} (see Fig. 2). The diminishment of τ_{eff} can be attributed to the increase of the oxygen concentration in the a-SiO_xN_y:H films, which is accompanied by an increase of the bulk defect density [18]. This in turn determines the density of interface traps D_{it} between amorphous and crystalline silicon in the equilibrium state [19] and thus decreases effective minority carrier lifetime.

Since the nitrogen concentration of the films investigated in this study is only one order of magnitude lower than the oxygen concentration, it is reasonable to speak of amorphous silicon oxynitride films instead of silicon oxide films.

b) FTIR analysis

The bonding structure of the a-SiO_xN_y:H films is investigated qualitatively by means of Fourier-Transform Infrared (FTIR) spectroscopy.

An almost linear shift of the center of the Si-O-Si stretching mode peak (1005 cm^{-1} at R_{N2O} = 10%) towards higher wavenumbers is observable with increasing N_2O gas dilution ratio (1020 cm^{-1} at R_{N2O} = 33%) (Fig. 6). This shift is simply related to the oxygen content in the film [20]. The frequency of an isolated Si-O-Si bond in an a-Si:H network is 940 cm^{-1}, whereas the frequency shifts to 1080 cm^{-3} for a Si-O-Si bond in a-SiO_2 [20].

The linearity of the frequency shift reveals a random distribution of Si-Si and Si-O-Si bonds in the a-SiO_xN_y:H film [21]. Beside the peak position shift of the Si-O-Si bond stretching mode, two other peaks located at around 2000 cm^{-1} and 2060 cm^{-1} shift towards higher wavenumbers with increasing N_2O gas dilution ratio (Fig. 6). Both peaks originate from Si-H bond stretching vibrations of a monohydride bonding arrangement.

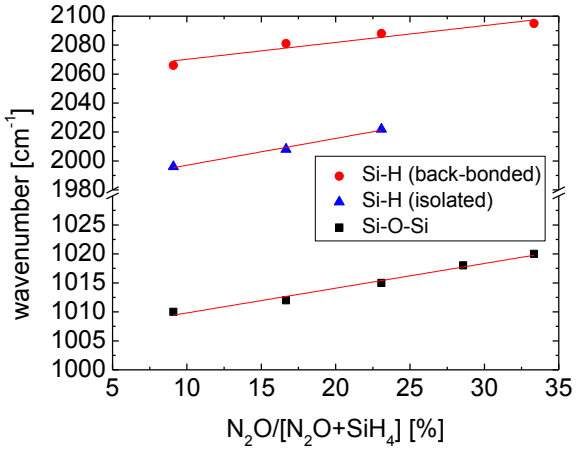

Figure 6: Peak position of Si-O-Si and Si-H stretching mode vibrations of a-SiO_xN_y:H films as a function of N_2O gas dilution ratio.

The absorption peak at around 2000 cm^{-1} is caused by Si-H bonds, in which the Si atom has only Si neighbors [22], whereas the peak at 2060 cm^{-1} can be attributed to Si-H stretching vibrations, in which one of the atoms back-bonded to the silicon is an oxygen atom [23].

The already discussed shift of both peaks towards higher wavenumbers with increasing N_2O gas flow originates from an enhanced electro-negativity of the neighbors being more distant from the Si-H bond [23]. Thus, more oxygen atoms are incorporated in the amorphous network with increasing N_2O gas flow. Furthermore, the intensity of the isolated Si-H peak decreases with increasing N_2O gas flow ratio for the benefit of the intensity of the Si-H peak which is back-bonded to an oxygen atom (not depicted), meaning again that more oxygen atoms are incorporated in the a-SiO_xN_y:H film with increasing N_2O gas dilution ratio.

4 CONCLUSION

We have studied the applicability of low temperature (T_{dep} <200°C) Si-rich amorphous silicon oxynitride (a-SiO_xN_y:H) films for crystalline silicon solar cells. The passivation quality as well as the optical properties of the a-SiO_xN_y:H films grown by plasma decomposition (PECVD) of silane and nitrous oxide have been investigated.

We have shown that the optical band gap, the passivation quality and the refractive indices of the films are well correlated with the oxygen concentration. The latter in turn strongly depends on the deposition parameters. Both minority carrier lifetime and optical band gap depend linearly on the N_2O gas dilution ratio, but inversely to each other.

In order to maximize effective minority carrier lifetime, a deposition temperature of 175°C and a high deposition power revealed to be the optimum parameters if a post-deposition annealing step at 300°C follows. When applying an a-SiO_xN_y:H film with an optical gap of 2.0 eV, a very low effective surface recombination velocity of 5 cm/s (τ_{eff} = 2.5 ms) on a 2 Ωcm p-type FZ wafer could be measured.

In general, the manufacturing of Si-rich a-SiO_xN_y:H films is similar to the one of amorphous silicon films, i.e. grown by low temperature plasma enhanced chemical vapor deposition. Effective minority carrier lifetimes are comparable to a-Si:H films, but these films suffer less from parasitic absorption over the whole wavelength range because of their higher optical band gap. Ongoing with this fact is the possibility to tune the refraction index in a certain range, which turns amorphous silicon oxynitride into a very interesting material for solar cell applications, in particular for heterojunction solar cells and multilayer anti reflection coatings.

5 ACKNOWLEDGEMENTS

We would like to thank A. Herguth for fruitful discussions as well as S. Wilking and B. Rettenmaier for technical support. We gratefully acknowledge the sponsorship by the scholarship programme of the German Federal Environmental Foundation (Deutsche Bundesstiftung Umwelt, DBU). The financial support from the BMU project FKZ 0325079 is gratefully acknowledged in particular for the processing equipment. The content of this publication is the responsibility of the authors.

6 REFERENCES

[1] A. Aberle, Crystalline Silicon Solar Cells – Advanced Surface Passivation and Analysis, UNSW (1999)
[2] S. Dauwe et al., Proc. 29th IEEE PVSC (2002) 1246.
[3] H. Plagwitz, PhD Thesis, G.W. Leibniz University of Hannover (2007)
[4] R.A. Street, Hydrogenerated Amorphous Silicon, Cambridge University Press (1990)
[5] D. Suwito, PhD Thesis, University of Konstanz (2011)
[6] T. Mueller et al., J. Appl. Phys. **107** (2010) 014504.
[7] A. Laades et al., Proc. 26th EUPVSEC (2011) 1653.
[8] J. Seiffe et al., J. Appl. Phys. **109** (2011) 034105.
[9] F.A. Bogenschuetz, Aetzpraxis fuer Halbleiter, Hanser (1967)
[10]W. Kern, J. Electrochem. Soc. **137** (1990) 6
[11]R.A. Sinton et al. Appl. Phys. Lett. **69** (1996) 2510
[12]A.B. Sproul, J. Appl. Phys. **76** (1994) 2851
[13] Staebler et al., J. Appl. Phys. **51**, (1980)
[14]M. Fox, Optical Properties of Solids, Oxford University Press (2010)
[15]J. Tauc et al., J. Non-Crystl. Solids **8** (1972) 569
[16]H. Plagwitz et al., J. Appl. Phys. **103** (2008) 94506.
[17]M.I. Alayo et al., Thin Solid Films **402** (2002) 154.
[18]A. Janotta et al., Phys. Rev. B **69** (2004) 115206.
[19]T.F. Schulze et al., Appl. Phys. Lett. **96** (2010) 252102.
[20]G. Lucovsky et al., Phys. Rev. B **28** (1983) 3225.
[21]K. Haga et al., J. of Non-Cryst. Solids **195** (1996) 72.
[22]D.V. Tsu et al., Phys. Rev. B **40** (1989) 1795.
[23]G.N. Parsons et al., Phys. Rev. B **41** (1990) 1664.